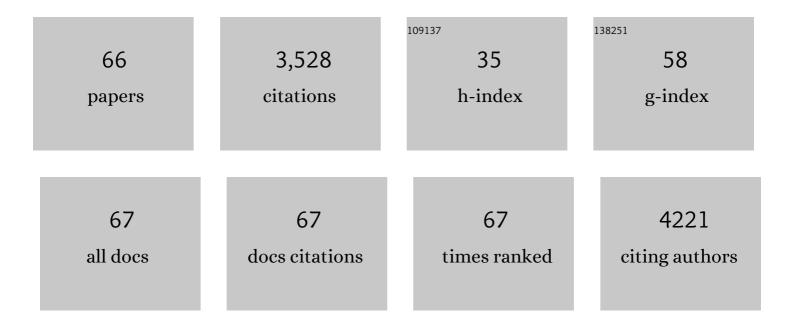
Joseph A O'donoghue

List of Publications by Year in descending order

Source: https://exaly.com/author-pdf/3717576/publications.pdf Version: 2024-02-01



LOSEDH & O'DONOCHUE

#	Article	IF	CITATIONS
1	[89Zr]Zr-huJ591 immuno-PET targeting PSMA in IDH mutant anaplastic oligodendroglioma. European Journal of Nuclear Medicine and Molecular Imaging, 2022, 49, 783-785.	3.3	4
2	Theranostics: The Role of Quantitative Nuclear Medicine Imaging. Seminars in Radiation Oncology, 2021, 31, 28-36.	1.0	10
3	Improved image reconstruction of 89Zr-immunoPET studies using a Bayesian penalized likelihood reconstruction algorithm. EJNMMI Physics, 2021, 8, 6.	1.3	7
4	First-in-Humans Imaging with ⁸⁹ Zr-Df-IAB22M2C Anti-CD8 Minibody in Patients with Solid Malignancies: Preliminary Pharmacokinetics, Biodistribution, and Lesion Targeting. Journal of Nuclear Medicine, 2020, 61, 512-519.	2.8	170
5	Comparison of 68Ga-DOTA-JR11 PET/CT with dosimetric 177Lu-satoreotide tetraxetan (177Lu-DOTA-JR11) SPECT/CT in patients with metastatic neuroendocrine tumors undergoing peptide receptor radionuclide therapy. European Journal of Nuclear Medicine and Molecular Imaging, 2020, 47, 3047-3057.	3.3	19
6	Safety and Feasibility of PARP1/2 Imaging with 18F-PARPi in Patients with Head and Neck Cancer. Clinical Cancer Research, 2020, 26, 3110-3116.	3.2	36
7	CD38-targeted Immuno-PET of Multiple Myeloma: From Xenograft Models to First-in-Human Imaging. Radiology, 2020, 295, 606-615.	3.6	73
8	Phase I Trial of Well-Differentiated Neuroendocrine Tumors (NETs) with Radiolabeled Somatostatin Antagonist 177Lu-Satoreotide Tetraxetan. Clinical Cancer Research, 2019, 25, 6939-6947.	3.2	69
9	Retooling a Blood-Based Biomarker: Phase I Assessment of the High-Affinity CA19-9 Antibody HuMab-5B1 for Immuno-PET Imaging of Pancreatic Cancer. Clinical Cancer Research, 2019, 25, 7014-7023.	3.2	47
10	⁸⁹ Zr-Immuno-PET: Toward a Noninvasive Clinical Tool to Measure Target Engagement of Therapeutic Antibodies In Vivo. Journal of Nuclear Medicine, 2019, 60, 1825-1832.	2.8	38
11	Pharmacokinetics and Biodistribution of a [⁸⁹ Zr]Zr-DFO-MSTP2109A Anti-STEAP1 Antibody in Metastatic Castration-Resistant Prostate Cancer Patients. Molecular Pharmaceutics, 2019, 16, 3083-3090.	2.3	26
12	lmaging Patients with Metastatic Castration-Resistant Prostate Cancer Using ⁸⁹ Zr-DFO-MSTP2109A Anti-STEAP1 Antibody. Journal of Nuclear Medicine, 2019, 60, 1517-1523.	2.8	38
13	Biodistribution and radiation dose estimates for 68Ga-DOTA-JR11 in patients with metastatic neuroendocrine tumors. European Journal of Nuclear Medicine and Molecular Imaging, 2019, 46, 677-685.	3.3	44
14	Copper-64 trastuzumab PET imaging: a reproducibility study. Quarterly Journal of Nuclear Medicine and Molecular Imaging, 2019, 63, 191-198.	0.4	21
15	Pharmacokinetics, Biodistribution, and Radiation Dosimetry for ⁸⁹ Zr-Trastuzumab in Patients with Esophagogastric Cancer. Journal of Nuclear Medicine, 2018, 59, 161-166.	2.8	96
16	First-in-Human Human Epidermal Growth Factor Receptor 2–Targeted Imaging Using ⁸⁹ Zr-Pertuzumab PET/CT: Dosimetry and Clinical Application in Patients with Breast Cancer. Journal of Nuclear Medicine, 2018, 59, 900-906.	2.8	126
17	I-124 codrituzumab imaging and biodistribution in patients with hepatocellular carcinoma. EJNMMI Research, 2018, 8, 20.	1.1	17
18	Multiparametric Imaging of Tumor Hypoxia and Perfusion with ¹⁸ F-Fluoromisonidazole Dynamic PET in Head and Neck Cancer. Journal of Nuclear Medicine, 2017, 58, 1072-1080.	2.8	31

#	Article	IF	CITATIONS
19	Bombesin Antagonist-Based Radiotherapy of Prostate Cancer Combined with WST-11 Vascular Targeted Photodynamic Therapy. Clinical Cancer Research, 2017, 23, 3343-3351.	3.2	19
20	Monitoring early response to chemoradiotherapy with 18F-FMISO dynamic PET in head and neck cancer. European Journal of Nuclear Medicine and Molecular Imaging, 2017, 44, 1682-1691.	3.3	33
21	First-in-Human Imaging with ⁸⁹ Zr-Df-IAB2M Anti-PSMA Minibody in Patients with Metastatic Prostate Cancer: Pharmacokinetics, Biodistribution, Dosimetry, and Lesion Uptake. Journal of Nuclear Medicine, 2016, 57, 1858-1864.	2.8	116
22	Cerenkov Luminescence Imaging for Radiation Dose Calculation of a ⁹⁰ Y-Labeled Gastrin-Releasing Peptide Receptor Antagonist. Journal of Nuclear Medicine, 2015, 56, 805-811.	2.8	39
23	A Phase I/II Study for Analytic Validation of 89Zr-J591 ImmunoPET as a Molecular Imaging Agent for Metastatic Prostate Cancer. Clinical Cancer Research, 2015, 21, 5277-5285.	3.2	163
24	Indium 111-labeled J591 anti-PSMA antibody for vascular targeted imaging in progressive solid tumors. EJNMMI Research, 2015, 5, 28.	1.1	63
25	PET-based compartmental modeling of 124I-A33 antibody: quantitative characterization of patient-specific tumor targeting in colorectal cancer. European Journal of Nuclear Medicine and Molecular Imaging, 2015, 42, 1700-1706.	3.3	13
26	A Recommendation for Revised Dose Calibrator Measurement Procedures for 89Zr and 124I. PLoS ONE, 2014, 9, e106868.	1.1	20
27	89Zr-huJ591 immuno-PET imaging in patients with advanced metastatic prostate cancer. European Journal of Nuclear Medicine and Molecular Imaging, 2014, 41, 2093-2105.	3.3	130
28	Radiation Safety Considerations for the Use of 223RaCl2 DE in Men with Castration-resistant Prostate Cancer. Health Physics, 2014, 106, 494-504.	0.3	59
29	Pilot study of PET imaging of 124I-iodoazomycin galactopyranoside (IAZGP), a putative hypoxia imaging agent, in patients with colorectal cancer and head and neck cancer. EJNMMI Research, 2013, 3, 42.	1.1	12
30	Phase I pharmacokinetic and biodistribution study with escalating doses of 223Ra-dichloride in men with castration-resistant metastatic prostate cancer. European Journal of Nuclear Medicine and Molecular Imaging, 2013, 40, 1384-1393.	3.3	160
31	Pilot study of 68Ga-DOTA-F(ab′)2-trastuzumab in patients with breast cancer. Nuclear Medicine Communications, 2013, 34, 1157-1165.	0.5	68
32	Image-Guided Po ₂ Probe Measurements Correlated with Parametric Images Derived from ¹⁸ F-Fluoromisonidazole Small-Animal PET Data in Rats. Journal of Nuclear Medicine, 2012, 53, 1608-1615.	2.8	34
33	Dosimetric Analysis of ¹⁷⁷ Lu-cG250 Radioimmunotherapy in Renal Cell Carcinoma Patients: Correlation with Myelotoxicity and Pretherapeutic Absorbed Dose Predictions Based on ¹¹¹ In-cG250 Imaging. Journal of Nuclear Medicine, 2012, 53, 82-89.	2.8	45
34	Bone Marrow Dosimetry Using ¹²⁴ I-PET. Journal of Nuclear Medicine, 2012, 53, 615-621.	2.8	26
35	18F-Fluromisonidazole PET Imaging as a Biomarker for the Response to 5,6-Dimethylxanthenone-4-Acetic Acid in Colorectal Xenograft Tumors. Journal of Nuclear Medicine, 2011, 52, 437-444.	2.8	31
36	¹²⁴ I-huA33 Antibody PET of Colorectal Cancer. Journal of Nuclear Medicine, 2011, 52, 1173-1180.	2.8	85

#	Article	IF	CITATIONS
37	Correlation of In Vivo and In Vitro Measures of Carbonic Anhydrase IX Antigen Expression in Renal Masses Using Antibody 124I-cG250. Journal of Nuclear Medicine, 2011, 52, 535-540.	2.8	47
38	¹²⁴ I-huA33 Antibody Uptake Is Driven by A33 Antigen Concentration in Tissues from Colorectal Cancer Patients Imaged by Immuno-PET. Journal of Nuclear Medicine, 2011, 52, 1878-1885.	2.8	47
39	Detection of hypoxia in microscopic tumors using 1311-labeled iodo-azomycin galactopyranoside (1311-IAZGP) digital autoradiography. European Journal of Nuclear Medicine and Molecular Imaging, 2010, 37, 339-348.	3.3	24
40	High ¹⁸ F-FDG Uptake in Microscopic Peritoneal Tumors Requires Physiologic Hypoxia. Journal of Nuclear Medicine, 2010, 51, 632-638.	2.8	38
41	Phase I Study of Samarium-153 Lexidronam With Docetaxel in Castration-Resistant Metastatic Prostate Cancer. Journal of Clinical Oncology, 2009, 27, 2436-2442.	0.8	92
42	Radiosynthesis of [1311]IAZGP via nucleophilic substitution and its biological evaluation as a hypoxia marker — is specific activity a factor influencing hypoxia-mapping ability of a hypoxia marker?. Nuclear Medicine and Biology, 2009, 36, 477-487.	0.3	10
43	In vivo characterization of a reporter gene system for imaging hypoxia-induced gene expression. Nuclear Medicine and Biology, 2009, 36, 821-831.	0.3	15
44	Noninvasive Multimodality Imaging of the Tumor Microenvironment: Registered Dynamic Magnetic Resonance Imaging and Positron Emission Tomography Studies of a Preclinical Tumor Model of Tumor Hypoxia. Neoplasia, 2009, 11, 247-IN3.	2.3	107
45	Preclinical radioimmunotargeting of folate receptor alpha using the monoclonal antibody conjugate DOTA–MORAb-003. Nuclear Medicine and Biology, 2008, 35, 343-351.	0.3	42
46	Hypoxia in microscopic tumors. Cancer Letters, 2008, 264, 172-180.	3.2	60
47	Antibody Mass Escalation Study in Patients with Castration-Resistant Prostate Cancer Using ¹¹¹ In-J591: Lesion Detectability and Dosimetric Projections for ⁹⁰ Y Radioimmunotherapy. Journal of Nuclear Medicine, 2008, 49, 1066-1074.	2.8	76
48	Image deconvolution in digital autoradiography: A preliminary study. Medical Physics, 2008, 35, 522-530.	1.6	11
49	Phase I Evaluation of J591 as a Vascular Targeting Agent in Progressive Solid Tumors. Clinical Cancer Research, 2007, 13, 2707-2713.	3.2	73
50	Visualization of Hypoxia in Microscopic Tumors by Immunofluorescent Microscopy. Cancer Research, 2007, 67, 7646-7653.	0.4	111
51	Measurements of Partial Oxygen Pressure (pO2) using the OxyLite System in R3327-AT Tumors under Isoflurane Anesthesia. Radiation Research, 2006, 166, 512-518.	0.7	16
52	Assessment of regional tumor hypoxia using 18F-fluoromisonidazole and 64Cu(II)-diacetyl-bis(N4-methylthiosemicarbazone) positron emission tomography: Comparative study featuring microPET imaging, Po2 probe measurement, autoradiography, and fluorescent microscopy in the R3327-AT and FaDu rat tumor models. International Journal of Radiation Oncology Biology Physics,	0.4	183
53	2005, 61, 1493-1502. Pilot Trial of Unlabeled and Indium-111–Labeled Anti–Prostate-Specific Membrane Antigen Antibody J591 for Castrate Metastatic Prostate Cancer. Clinical Cancer Research, 2005, 11, 7454-7461.	3.2	120
54	Cell line-dependent differences in uptake and retention of the hypoxia-selective nuclear imaging agent Cu-ATSM. Nuclear Medicine and Biology, 2005, 32, 623-630.	0.3	98

JOSEPH A O'DONOGHUE

#	Article	IF	CITATIONS
55	Relevance of External Beam Dose–Response Relationships to Kidney Toxicity Associated with Radionuclide Therapy. Cancer Biotherapy and Radiopharmaceuticals, 2004, 19, 378-387.	0.7	36
56	Phase I clinical trial with fractionated radioimmunotherapy using 131I-labeled chimeric G250 in metastatic renal cancer. Journal of Nuclear Medicine, 2004, 45, 1412-21.	2.8	72
57	A stereotactic method for the three-dimensional registration of multi-modality biologic images in animals: NMR, PET, histology, and autoradiography. Medical Physics, 2003, 30, 2303-2314.	1.6	52
58	Hematologic Toxicity in Radioimmunotherapy: Dose-Response Relationships for I-131 Labeled Antibody Therapy. Cancer Biotherapy and Radiopharmaceuticals, 2002, 17, 435-443.	0.7	44
59	Iodination of annexin V for imaging apoptosis. Journal of Nuclear Medicine, 2002, 43, 671-7.	2.8	33
60	Tumor Burden Assessment with Positron Emission Tomography with [18-F] 2-fluoro 2-deoxyglucose (FDG PET) Modeled in Metastatic Renal Cell Cancer. Molecular Imaging and Biology, 2000, 3, 57-65.	0.3	24
61	Changes in FDG Tumor Uptake during and after Fractionated Radiation Therapy in a Rodent Tumor Xenograft. Molecular Imaging and Biology, 1999, 2, 289-296.	0.3	8
62	Mathematical model of 5-[125I]iodo-2′-deoxyuridine treatment: continuous infusion regimens for hepatic metastases. International Journal of Radiation Oncology Biology Physics, 1998, 41, 1177-1183.	0.4	6
63	Calculation of integrated biological response in brachytherapy. International Journal of Radiation Oncology Biology Physics, 1997, 38, 633-642.	0.4	53
64	Optimum combination of targeted 131I and total body irradiation for treatment of disseminated cancer. International Journal of Radiation Oncology Biology Physics, 1995, 32, 713-721.	0.4	5
65	The Impact of Tumor Cell Proliferation in Radioimmunotherapy. Cancer, 1994, 73, 974-980.	2.0	31
66	The effect on human neuroblastoma spheroids of fractionated radiation regimes calculated to be equivalent for damage to late responding normal tissues. European Journal of Cancer & Clinical Oncology, 1987, 23, 855-860.	0.9	6